Shape coexistence in ^{71}Br and the question of the ground-state spin of ^{71}Kr

S. M. Fischer*
Department of Physics, DePaul University, Chicago, Illinois 60614, USA and Physics Division, Argonne National Laboratory, Argonne, Illinois 60439, USA

T. Anderson, P. Kerns, G. Mesoloras, and D. Svelnys†
Department of Physics, DePaul University, Chicago, Illinois 60614, USA

C. J. Lister
Physics Division, Argonne National Laboratory, Argonne, Illinois 60439, USA

D. P. Balamuth and P. A. Hausladen‡
Department of Physics and Astronomy, University of Pennsylvania, Philadelphia, Pennsylania 19104, USA

D. G. Sarantites
Department of Chemistry, Washington University, St. Louis, Missouri 63130, USA
(Received 6 May 2005; published 31 August 2005)

When the $N = Z$ line approaches the proton dripline above ^{56}Ni an increasing distortion of mirror symmetry is expected as the proton-rich partner becomes marginally bound. Urkedal and Hamamoto have considered ^{71}Kr and suggest the distortion could lead to a different ground-state spin to its mirror partner ^{71}Br, based on the reinterpretation of a β-decay measurement. This would be a unique situation in $T = 1/2$ nuclei. We have performed a new in-beam spectroscopic measurement of ^{71}Br, following the ^{40}Ca(^{40}Ca,2αp) reaction at 160 MeV and using Gammasphere. Many new states have been found, with candidates for eight Nilsson bandheads below 1 MeV. Cross-linking decays tightly constrain most of the angular momentum assignments. The ^{71}Kr β-decay data, seen in the light of this new information on ^{71}Br, support the original ground-state assignment of ^{71}Kr as $J^\pi = 5/2^-$, as would be normally expected for the mirror partner of $J^\pi = 5/2^-$ ^{71}Br.

DOI: 10.1103/PhysRevC.72.024321 PACS number(s): 21.10.Hw, 23.20.En, 23.20.Lv, 27.50.+e

I. INTRODUCTION

The question of Coulomb distortion of mirror symmetry and the demise of the isospin quantum number has been a long-standing topic in nuclear structure. Many years ago, Ehrman and Thomas [1,2] suggested that unbound proton states in the $T_z = -1/2$ nucleus ^{13}N had a radially extended wave-function and thus lower Coulomb energies than its more tightly bound $T_z = +1/2$ ^{13}C counterpart. Because the size of the shift depends on the radial wave-function, inversions of the sequence of states are possible. The original interest focused on highly excited states in nuclei near stability, but this type of effect should be found close to the ground state of nuclei beyond the proton dripline. In heavier $N = Z$ nuclei the Coulomb energy rises, the binding energy falls, and the proton dripline is approached, so the feature should eventually become ubiquitous despite the ever stiffening barrier that holds in the poorly bound proton wave-functions. Suitable candidates with low binding energy lie in $N \sim Z$ nuclei with $A \sim 70$; for example, the ^{69}Br ground state is proton unbound by $\approx$500 keV with a half-life of $\leqslant$24 ns [3,4] whereas its $T_z = +1/2$ counterpart ^{69}Se is bound and has a half-life of 27.4 s [5]. To complicate matters in the $A \sim 70$ region, oblate-prolate shape coexistence is well known [6,7]. The Coulomb energy is sensitive to shape [8], so mirror partners may have significant shifts in the relative excitation energy of different shapes. Taken together, at some point, the assumption that the ground-state spin of a less bound $T_z = -1/2$ nucleus is always the same as its more bound $T_z = +1/2$ mirror partner must come into question and will probably be violated somewhere.

Urkedal and Hamamoto [9] used arguments of this type to suggest that an example where the ground-state spins of a mirror pair are different already exists; specifically they suggested that the ground-state spin of ^{71}Kr may be $J^\pi = 3/2^-$ and not $J^\pi = 5/2^-$, which is known for its mirror partner, ^{71}Br, and which was originally proposed in the experiment that investigated ^{71}Kr [10]. To reach this conclusion, Urkedal and Hamamoto suggested a new set of angular momentum assignments for the few states that were known [11] in ^{71}Br and then reinterpreted the β decay of ^{71}Kr. In the present study, we have performed a new experiment on ^{71}Br and have greatly extended and improved the spectroscopic information. We have discovered a complex decay scheme with many interlinked bands that tightly constrain most spin assignments

*Corresponding Author: sfischer@depaul.edu
†Permanent address: Rickover Naval Academy, 5900 N. Glenwood, Chicago, Illinois 60660, USA.
‡Permanent address: P.O. Box 2008, Oak Ridge National Laboratory, Oak Ridge, Tennessee 37831-6010, USA.

and allow this specific issue of mirror symmetry to be clarified. Our rather complete set of bandheads reveals oblate-prolate shape coexistence as is found in neighboring nuclei.

Relatively little was known about excited states in ^{71}Br prior to this work. In 1990, Arrison *et al.* [11] published the first spectroscopic investigation of low-lying states in ^{71}Br; more recently Martinez *et al.* [12] considerably extended the decay scheme in an unpublished work. The only report on the β spectroscopy of ^{71}Kr to states in ^{71}Br is by Oinonen *et al.* [10].

II. THE EXPERIMENT

^{71}Br was quite strongly produced ($\sigma \sim 10$ mb, or about 2% of the residues) in the ^{40}Ca(^{40}Ca,2αp) reaction at 160 MeV in a large data set aimed at studying nuclei with $N = Z$ [13,14]. The beams were provided by the ATLAS accelerator, from the ECRII injector, then stripped and accelerated to the $q = 19$ charge state to avoid any contamination from ^{40}Ar, which cannot form ions above $q = 18$. The high efficiency of Gammasphere [15] provided data of excellent statistical quality that allowed a detailed spectroscopic investigation. A thin target of isotopically enriched ^{40}Ca ($\approx$500 μg/cm^2 on a 120 μg/cm^2 gold backing with a 90 μg/cm^2 gold cover to prevent oxidation) was used, so residues escaped from the target at approximately uniform velocity along the beam direction. The experiment used Microball [16] to detect and measure the energies of evaporated protons and α particles. Determination of the momenta of the evaporated particles allowed event-by-event Doppler corrections to be applied. Data were collected in which at least four γ rays were detected in coincidence with a charged particle and were collected for the equivalent of two days with an average beam current of 3.2 pnA.

The γ-ray data were sorted a number of different ways. A RadWare cube [17] was constructed with the requirement that two α particles and one proton were identified in the Microball array. No subtraction of breakthrough from the $2\alpha 2p$ channel (^{70}Se) was applied to the data in the cube, but the requirement of two γ gates produced quite clean spectra. Two-dimensional $\gamma\gamma$ matrices for events corresponding to the detection of $2\alpha 1p$ and $2\alpha 2p$ were also obtained. Single gates applied to the $2\alpha 1p$ matrix were corrected for background resulting from the breakthrough of the $2\alpha 2p$ channel, and provided a check for spectra obtained from $\gamma\gamma$ gates applied to the cube. The level scheme was built primarily from these two sorts.

Transition multipolarities and angular momentum assignments for the levels were determined by examining gated γ-ray angular distributions. Because of the large number of doublets observed for ^{71}Br, the distributions were obtained by gating on a series of γ-ray transitions detected at all angles, and then looking at the coincident γ rays that were detected in specific rings of the Gammasphere array. A channel subtraction was performed on the angular distribution data to remove the $2\alpha 2p$ contribution. The gating procedure limited the statistics for the distributions, making it advantageous to add together clusters of detectors from neighboring rings. This was particularly important for producing angular distribution

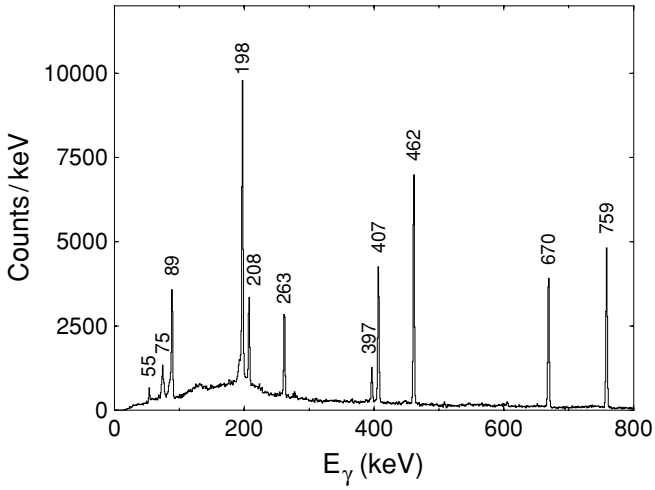

FIG. 1. A projection of delayed γ rays following prompt detection of at least one γ ray, two α particles, and a proton. The events are selected 30–110 ns after a beam burst and appear to be almost entirely due to ^{71}Br without any further manipulation. The $\sim$75-keV x ray arises from fluorescence of lead and bismuth in Gammasphere.

spectra for transitions in ^{71}Br that lie below the known isomeric state at 759 keV, which has a half-life of 33 ns [11]. Most of these transitions are fed from states both above and below the isomer. Gating on transitions that bypass the isomer ensured that the state being studied retained the alignment produced in the reaction and allowed for reliable extraction of angular momenta and multipolarities.

The existence of the 33-ns isomer allowed additional analyses of the data involving delayed γ rays. Prompt evaporated particles leading to ^{71}Br were identified in Microball, followed by delayed γ rays observed in a time window of 30–110 ns after the accelerator beam bursts that occurred every 82 ns and were $\sim$5 ns wide. These delayed γ rays were emitted from nuclei that had recoiled from the target off-axis owing to the 2α evaporation and were caught on the inside surface of Microball, so remained partially in the field of view of some Gammasphere detectors. Unlike the prompt radiation, these delayed transitions had no Doppler shifts, nor continuum cooling radiation. Matrices of prompt versus delayed γ rays and delayed versus delayed γ rays were constructed. The combination of channel selection through prompt evaporated charged particles followed by the isomer timing, and the lack of any Doppler effect, make these data extremely clean, containing only γ rays from below the isomer in ^{71}Br, with the exception of a 75-keV x ray from fluorescence of lead and bismuth in Gammasphere. Figure 1 shows the projection of the $\gamma\gamma$ matrix of transitions with one prompt and one delayed γ ray cleanly showing the stopped decays from below the isomer.

III. ANALYSIS AND SPIN ASSIGNMENTS

Excited states in ^{71}Br were first reported by Arrison *et al.* [11] using unsuppressed germanium counters triggered

by neutron detectors following the ^{58}Ni(^{16}O,$p2n$)^{71}Br reaction. They constructed a decay scheme with 10 states that contains all the strongest transitions we find in the present study, including the crucial decay of the $T_{1/2} = 32.5$ ns, $J^{\pi} = 9/2^{+}$ isomer at 759 keV. More recently, the Legnaro group [12] extended the decay scheme by 25 more levels in an unpublished report. In this work we have made considerable further progress, adding many transitions and levels. More than 100 transitions are placed in the decay scheme and are listed in Table I. Our data were of sufficient quality that the angular distributions of many transitions could be measured, allowing the spins and parities of most low-lying levels to be unambiguously assigned. This is a complicated decay scheme and interpreting it depends strongly on these assignments. We have also made alterations to the previous decay schemes [11,12], which are important and require discussion individually. These changes are critical for the issue of ^{71}Kr β decay discussed in Sec. IV A.

It is instructive to begin by examining the states below the isomer. Coincidences between pairs of delayed transitions were essentially background-free and even a few counts in a peak are enough to demonstrate a coincidence. The key new finding is that there are three unambiguous γ-ray doublets among the low-lying transitions. The 407-keV photopeak actually contains two separate decays, as does the 198/199-keV peak and the 208-keV peak. These doublets are a surprising and previously unsuspected feature in the data that led to the original misinference of a 262-keV level [11]. The doublet nature of the 407-keV peak was first noted in the Legnaro study [12].

The panels in Fig. 2 show the relevant delayed $\gamma\gamma$ coincidence spectra, and the low-lying energy levels deduced from this work are displayed in Fig. 3, with details given in Table I. Figure 2(a) shows a delayed gate on the 198/199-keV photopeak, which clearly indicates that the 263-keV transition is in coincidence, in contradiction with [11]. There is evidence for a 199-keV self-coincident peak, and a single 407-keV line is observed with no evidence for a peak at 397 keV. Reversing the sort and gating on the 263-keV peak [Fig. 2(b)] shows even more clearly the 198/199 coincidence, but also evidence of a 407-keV level with decays by 407- and 397-keV transitions to the ground state and 10-keV level. A gate on the 397-keV line [Fig. 2(c)] reveals the placement of the upper 208-keV transition. Finally, a gate on the 208-keV doublet [Fig. 2(d)] again shows the two decays from the 407-keV level at 407 and 397 keV, along with a 198/199-keV coincidence that would not occur in the original scheme. These observations, together with our other coincidences and also Arrison's original data are all consistent with an inversion of the originally reported 262 $\rightarrow$ 407 keV cascade and the elimination of the proposed 262-keV state, which is now replaced by a level at 407 keV. We were not very sensitive to observation of a 55-keV transition in our current experiment, but neither was the original work [11], its presence being mainly inferred from coincidence relationships. However, in the delayed sort a 55-keV transition can still be clearly seen [Figs. 2(a) and 2(d)] that can be placed higher in excitation than originally suggested. Thus, all the original transitions of [11] are accounted for and retain their coincidence relationships, but taken with the additional

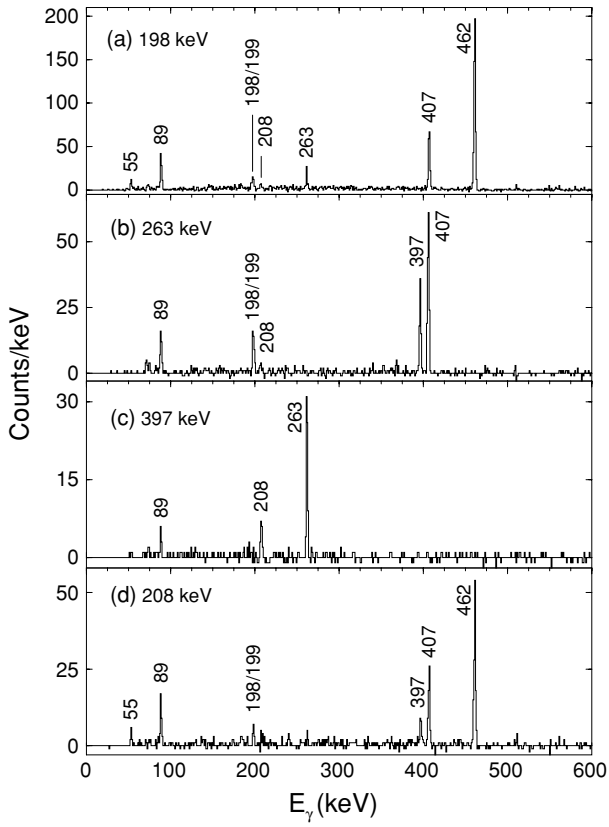

FIG. 2. A selection of delayed $\gamma\gamma$ coincidence spectra that reveal the true level structure of ^{71}Br. (a) A gate on the 198/199-keV line, showing self-coincidences and the clear presence of a 263-keV transition at higher energy. (b) A gate on the 263-keV line, showing one of the 407-keV transitions and the parallel 397-keV decay to the 10-keV state. (c) A gate on the 397-keV transition, revealing the placement of the upper 208-keV decay. (d) A gate on the 208-keV doublet, clearly showing 198/199 and 55-keV transitions.

information from the current experiment a new revised scheme can be rigorously demonstrated. The fragmentation of the

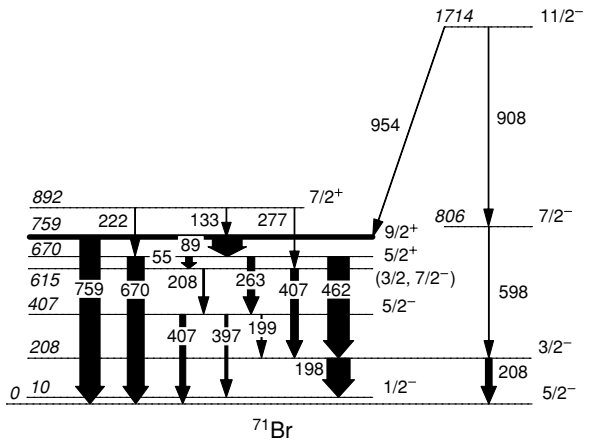

FIG. 3. The decay scheme of transitions de-exciting the $T_{1/2} =$ 33 ns $J^{\pi} = 9/2^{+}$ isomer in ^{71}Br, together with a few levels essential in establishing the spins of low-lying states.

TABLE I. The energy, angular momentum, and parity of the excited states of ^{71}Br, and the energy, relative intensity, and measured multipolarity of transitions from these states. The intensities were obtained from a spectrum of all γ rays measured in prompt coincidence with the detection of two α particles and one proton following the ^{40}Ca + ^{40}Ca reaction at 160 MeV. Feedthrough from the $2\alpha 2p$ channel was subtracted. The uncertainty in intensity corresponds to the statistical error in the fitted peak areas.

E_x (keV)	I_i^π	I_f^π	E_γ (keV)	Intensity	Multipolarity	δ
207.7(3)	$\frac{3}{2}^-$	$\frac{1}{2}^-$	198.0(2)	53.4(3)[a]	$M1/E2$	0.21(7)
		$\frac{5}{2}^-$	207.7(2)	16.0(3)[b]	$(E2)$	
407.2(3)	$\frac{5}{2}^-$	$\frac{3}{2}^-$	199.0(5)	53.4(3)[a]		
		$\frac{1}{2}^-$	397.2(2)	5.4(3)	$(E2)$	
		$\frac{5}{2}^-$	407.2(3)	15.9(4)[c]	$M1/E2$	−0.74(14)
614.9(4)	$(\frac{3}{2}, \frac{7}{2}^-)$	$\frac{5}{2}^-$	208.0(5)	16.0(3)[b]		
		$\frac{3}{2}^-$	407.2(3)	15.9(4)[c]		
669.7(3)	$\frac{5}{2}^+$	$(\frac{3}{2}, \frac{7}{2}^-)$	54.8(5)			
		$\frac{5}{2}^-$	262.5(3)	5.2(2)	$E1$	
		$\frac{3}{2}^-$	461.7(2)	13.6(2)	$E1$	
		$\frac{5}{2}^-$	669.5(2)	9.2(5)	$(E1)$	
722.0(3)	$(\frac{7}{2}^-)$	$\frac{3}{2}^-$	514.3(3)	15.5(3)		
759.1(3)	$\frac{9}{2}^+$	$\frac{5}{2}^+$	89.3(4)	40.4(12)		
		$\frac{5}{2}^-$	759.1(3)			
776.0(3)	$\frac{5}{2}^-$	$\frac{3}{2}^-$	568.3(4)	2.5(3)	$M1/E2$	0.03(9)
806.4(3)	$\frac{7}{2}^-$	$\frac{3}{2}^-$	598.7(3)	56.1(4)[d]	$E2$	
892.4(3)	$\frac{7}{2}^+$	$\frac{9}{2}^+$	133.2(3)	4.6(3)	$M1/E2$	0.02(16)
		$\frac{5}{2}^+$	222.4(3)	12.3(2)	$M1/E2$	0.12(5)
		$(\frac{3}{2}, \frac{7}{2}^-)$	276.5(5)	1.0(2)	$(E1)$	
929.4(3)	$\frac{7}{2}^-$	$\frac{5}{2}^-$	522.2(4)	11.5(3)		
		$\frac{3}{2}^-$	721.0(10)	6.7(3)		
		$\frac{5}{2}^-$	929.3(4)	10.2(6)		
1055.7(5)	$(\frac{9}{2}^-)$	$\frac{5}{2}^-$	1055.7(5)	11.4(9)		
1070.7(4)	$(\frac{7}{2}^-)$	$\frac{5}{2}^-$	663.4(4)	11.5(6)	$(M1/E2)$	0.24(7)
1174.2(3)	$\frac{9}{2}^+$	$\frac{7}{2}^+$	281.9(3)	4.8(2)	$M1/E2$	0.14(13)
		$\frac{9}{2}^+$	414.8(3)	11.4(3)	$M1/E2$	−0.51(35)
		$\frac{5}{2}^+$	504.5(3)	12.2(4)	$(E2)$	
1490.3(3)	$\frac{11}{2}^+$	$\frac{9}{2}^+$	316.1(3)	3.5(2)	$M1/E2$	0.02(13)
		$\frac{7}{2}^+$	598.0(4)	56.1(4)[d]	$E2$	
		$\frac{9}{2}^+$	731.2(4)	8.1(5)	$M1/E2$	0.64(8)
1491.9(3)	$\frac{9}{2}^-$	$\frac{7}{2}^-$	562.5(3)	16.8(3)	$M1/E2$	0.30(3)
1496.7(3)	$\frac{13}{2}^+$	$\frac{9}{2}^+$	737.6(3)	100	$E2$	
1586.2(4)	$\frac{11}{2}^+$	$\frac{9}{2}^+$	827.2(4)	7.5(4)		
1683.0(3)	$\frac{9}{2}^-$	$(\frac{7}{2}^-)$	613.4(4)	5.2(3)	$(E2)$	
		$\frac{5}{2}^-$	907.2(4)	45.3(6)[e]	$E2$	
1713.7(3)	$\frac{11}{2}^-$	$\frac{9}{2}^-$	222.4(3)	12.3(2)	$M1/E2$	0.23(10)
		$\frac{7}{2}^-$	907.7(4)	45.3(6)[e]	$E2$	
		$\frac{9}{2}^+$	954.2(5)	25.3(13)	$E1$	−0.03(7)

TABLE I. (*Continued*.)

E_x (keV)	I_i^π	I_f^π	E_γ (keV)	Intensity	Multipolarity	δ
		$(\frac{7}{2}^-)$	992.4(5)			
2122.0(3)	$\frac{13}{2}^+$	$\frac{11}{2}^+$	535.9(4)	3.5(3)		
		$\frac{13}{2}^+$	625.4(4)	1.6(2)	$M1/E2$	−0.42(70)
		$\frac{9}{2}^+$	947.8(4)	21.7(14)	$E2$	
2216.5(3)	$\frac{13}{2}^-$	$\frac{9}{2}^-$	724.5(5)	20.4(4)	$E2$	
		$(\frac{9}{2}^-)$	1161.3(4)	16.3(5)		
2217.4(3)	$\frac{13}{2}^+$	$\frac{11}{2}^+$	631.2(4)		$M1/E2$	0.06(9)
		$\frac{11}{2}^+$	727.0(5)			
2352.2(3)	$\frac{15}{2}^+$	$\frac{11}{2}^+$	861.9(4)	17.6(4)	$E2$	
2392.9(3)	$\frac{17}{2}^+$	$\frac{13}{2}^+$	896.2(3)	84.9(13)	$E2$	
2477.4(4)	$\frac{13}{2}^-$	$\frac{11}{2}^-$	762.8(4)	18.8(3)	$M1/E2$	0.27(5)
		$\frac{9}{2}^-$	794.5(5)	17.0(3)	$E2$	
2520.0(4)	$\frac{15}{2}^-$	$\frac{13}{2}^-$	303.4(5)	0.8(2)		
		$\frac{11}{2}^-$	806.0(3)	75.9(5)	$E2$	
3046.4(3)	$(\frac{17}{2}^+)$	$\frac{17}{2}^+$	653.8(4)			
		$\frac{15}{2}^+$	693.8(5)			
		$\frac{13}{2}^+$	829.9(5)	8.2(4)		
		$\frac{13}{2}^+$	924.6(5)		$(E2)$	
3187.9(4)	$\frac{17}{2}^-$	$\frac{13}{2}^-$	971.4(4)	31.1(5)	$E2$	
3262.0(3)	$\frac{17}{2}^+$	$\frac{17}{2}^+$	869.4(4)	2.8(4)		
		$\frac{13}{2}^+$	1139.8(5)	14.4(7)	$(E2)$	
3376.6(3)	$\frac{17}{2}^-$	$\frac{15}{2}^-$	857.1(4)	25.7(4)	$M1/E2$	−0.11(4)
		$\frac{13}{2}^-$	898.9(4)	18.8(19)	$E2$	
3433.8(4)	$\frac{19}{2}^+$	$\frac{15}{2}^+$	1081.6(4)	88.4(6)	$E2$	
3475.3(3)	$\frac{21}{2}^+$	$\frac{17}{2}^+$	1082.4(4)	88.4(6)	$E2$	
3529.1(3)	$\frac{19}{2}^-$	$\frac{15}{2}^-$	1009.4(3)	62.0(5)	$E2$	
4015.7(3)	$\frac{21}{2}^-$	$\frac{19}{2}^-$	486.8(3)	17.3(3)	$M1/E2$	−0.18
		$\frac{17}{2}^-$	638.8(3)	10.4(3)	$E2$	
4092.0(6)	$(\frac{21}{2}^+)$	$(\frac{17}{2}^+)$	1045.6(5)	15.4(4)	$E2$	
4310.9(3)	$\frac{21}{2}^-$	$\frac{19}{2}^-$	781.7(4)	11.2(3)	$M1/E2$	−0.06(6)
		$\frac{17}{2}^-$	934.2(4)	26.5(7)	$E2$	
		$\frac{17}{2}^-$	1123.3(4)	31.9(7)	$(E2)$	
4313.7(3)	$\frac{21}{2}^+$	$\frac{17}{2}^+$	1051.8(4)	13.2(9)	$E2$	
4503.1(4)	$\frac{25}{2}^+$	$\frac{21}{2}^+$	1027.8(4)	30.9(4)	$E2$	
4741.4(4)	$\frac{23}{2}^-$	$\frac{19}{2}^-$	1212.3(4)	47.8(6)	$E2$	
4743.7(4)	$\frac{25}{2}^+$	$\frac{21}{2}^+$	1268.4(4)	24.2(5)	$E2$	
4745.7(6)	$\frac{23}{2}^+$	$\frac{19}{2}^+$	1311.9(6)	19.0(6)	$E2$	
4969.4(3)	$\frac{25}{2}^+$	$\frac{21}{2}^+$	655.7(3)	17.7(4)	$E2$	
		$\frac{21}{2}^+$	1494.1(6)	16.6(9)	$E2$	
5313.5(5)	$(\frac{25}{2}^+)$	$(\frac{21}{2}^+)$	1221.5(4)	12.7(5)	$E2$	
5374.9(3)	$\frac{25}{2}^-$	$\frac{23}{2}^-$	633.1(3)	28.7(5)	$M1/E2$	−0.18(4)

TABLE I. (*Continued*.)

E_x (keV)	I_i^π	I_f^π	E_γ (keV)	Intensity	Multipolarity	δ
		$\frac{21}{2}^-$	1064.0(4)	44.7(4)	$E2$	
		$\frac{21}{2}^-$	1359.7(5)	24.5(7)	$E2$	
5811.8(4)	$\frac{29}{2}^+$	$\frac{25}{2}^+$	842.3(4)	19.9(3)	$E2$	
		$\frac{25}{2}^+$	1308.7(6)	16.7(7)	$E2$	
5994.6(5)	$\frac{27}{2}^+$	$\frac{23}{2}^+$	1248.9(4)	12.4(5)	$E2$	
6167.0(6)	$\frac{27}{2}^-$	$\frac{23}{2}^-$	1426.0(10)	16.3(7)	$E2$	
6190.9(5)	$\frac{29}{2}^+$	$\frac{25}{2}^+$	1447.2(5)	18.3(5	$E2$	
6613.5(4)	$\frac{29}{2}^-$	$\frac{27}{2}^-$	446.2(3)	2.0(2)	$M1/E2$	−0.36(13)
		$\frac{25}{2}^-$	1238.2(3)	59.2(6)	$E2$	
6709.0(6)	$(\frac{29}{2}^+)$	$(\frac{25}{2}^+)$	1395.5(5)	21.9(4)	$(E2)$	
7157.2(6)	$\frac{33}{2}^+$	$\frac{29}{2}^+$	1345.4(4)	33.6(6)	$E2$	
7425.0(10)		$\frac{27}{2}^-$	1258.0(10)			
7470.6(8)	$\frac{31}{2}^+$	$\frac{27}{2}^+$	1476.0(5)	18.1(8)	$(E2)$	
7759(2)	$(\frac{31}{2}^-)$	$\frac{27}{2}^-$	1591.9(15)			
7785.4(6)	$\frac{33}{2}^-$	$\frac{29}{2}^-$	1171.9(6)	48.0(7)	$E2$	
7790.0(10)	$\frac{33}{2}^+$	$\frac{29}{2}^+$	1599.0(8)	15.2(4)	$E2$	
8244.6(10)	$(\frac{33}{2}^+)$	$(\frac{29}{2}^+)$	1535.6(8)	7.2(4)	$(E2)$	
8423.0(10)		$\frac{33}{2}^-$	637.0(5)			
			998.0(5)			
8956(2)	$\frac{37}{2}^+$	$\frac{33}{2}^+$	1798.5(15)	29.1(5)	$E2$	
9090.2(10)	$\frac{35}{2}^+$	$\frac{31}{2}^+$	1619.6(8)	20.9(5)	$E2$	
9194.7(10)	$\frac{37}{2}^-$	$\frac{33}{2}^-$	1409.3(6)	18.1(4)	$E2$	
9320(2)	$(\frac{35}{2}^-)$	$(\frac{31}{2}^-)$	1561.3(15)			
9527(2)	$\frac{37}{2}^+$	$\frac{33}{2}^+$	1736.8(20)		$E2$	
9722(1)			1299(1)	23.3(7)		
9997(2)	$(\frac{37}{2}^+)$	$(\frac{33}{2}^+)$	1752(2)			
10752(2)	$(\frac{39}{2}^+)$	$\frac{35}{2}^+$	1661.7(15)	8.8(4)		
10993(2)	$(\frac{41}{2}^+)$	$\frac{37}{2}^+$	2036.7(15)	18.1(9)		
11031(2)	$(\frac{41}{2}^-)$	$\frac{37}{2}^-$	1836(2)	9.5(3)		
11434(2)	$(\frac{41}{2}^+)$	$\frac{37}{2}^+$	1907(2)			
11488(2)			1766(2)			
12381(2)	$(\frac{43}{2}^+)$	$(\frac{39}{2}^+)$	1629(2)			
12875(3)	$(\frac{45}{2}^+)$	$(\frac{41}{2}^+)$	1883(2)	11.7(6)		
13472(3)	$(\frac{45}{2}^+)$	$(\frac{41}{2}^+)$	2038(2)			
14959(3)	$(\frac{49}{2}^+)$	$(\frac{45}{2}^+)$	2084(2)			

[a]Combined intensity for the 198- and 199-keV transitions from levels at 208 and 407 keV, respectively.
[b]Combined intensity for the 208-keV transitions from levels at 208 and 615 keV.
[c]Combined intensity for the 407-keV transitions from levels at 407 and 615 keV.
[d]Combined intensity for the 599- and 598-keV transitions from levels at 806 and 1490 keV, respectively.
[e]Combined intensity for the 907- and 908-keV transitions from levels at 1683 and 1714 keV, respectively.

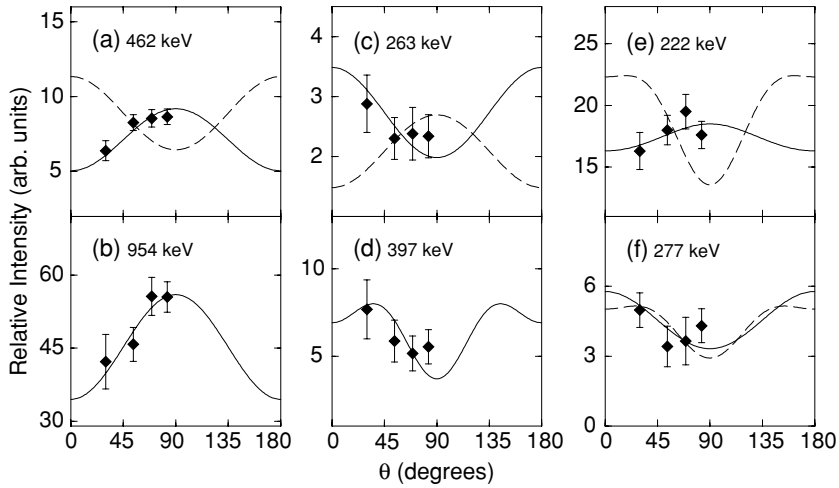

FIG. 4. A selection of angular distributions that were important in determining the spin sequences in ^{71}Br: (a) 462-keV $J^\pi = 5/2^+ \rightarrow 3/2^-$, (b) 954-keV $J^\pi = 11/2^- \rightarrow 9/2^+$, (c) 263-keV $J^\pi = 5/2^+ \rightarrow 5/2^-$, (d) 397-keV $J^\pi = 5/2^- \rightarrow 1/2^-$, (e) 222-keV $J^\pi = 7/2^+ \rightarrow 5/2^+$, and, (f) 277-keV $J^\pi = 7/2^+ \rightarrow 7/2^-$. Data for rings of detectors at similar forward and backward angles were combined in the analysis. See text for an explanation of the alternate spin hypotheses, shown as dashed lines.

isomeric decay to many low-spin states and the cleanliness of this data set suggest that the low-lying spectroscopy of ^{71}Br is essentially complete below 600 keV and it seems unlikely that there are more states to be found.

The firm assignment of spins and parities is crucial for the identification of bandheads, for inferring shapes, and for following how the bands evolve with rotation. The assignments are also important for interpreting the complicated band structure and for understanding the ^{71}Kr β decay. The measured angular distributions, taken together with the observed branching ratios, and recommended upper limits for transition strengths [18] have allowed the levels up to $\sim$1 MeV to be constrained in their possible spins and parities, in many cases without any ambiguity. It is frequently assumed that γ cascades following heavy-ion reactions are maximally "stretched." Although this assumption is often useful within a well-established band, it may break down for shell-model-type states, or when there is mixing between bands, as appears to be the case for ^{71}Br. For these reasons, we include the following discussion of the logic that constrains the spins and parities of all the low-lying states.

Radioactive decay [19] limits the ground-state spin of ^{71}Br to be $J^\pi = 3/2^-, 5/2^-$, or $7/2^-$. However, this is fixed at $J^\pi = 5/2^-$ by the characteristic $M2$ decay of the $J^\pi = 9/2^+, T_{1/2} = 33$ ns isomer at 759 keV [11]. The 89-keV decay from the isomer is $E2$ radiation, determined from the internal conversion coefficient [11], making the 670-keV level $J^\pi = 5/2^+$, as a $J^\pi = 13/2^+$ state would have no subsequent γ decay path. The properties of the 462-keV decay from the 670-keV state can be used to establish the angular momentum and parity of the 208-keV level. The solid curve in Fig. 4(a) shows the fitted angular distribution assuming a $5/2^+ \rightarrow 3/2$, pure $L = 1$ transition. In contrast, the dashed curve shows the poor agreement obtained for the $5/2^+ \rightarrow 5/2^-$ assignment for a pure $L = 1$ transition, as would be required for the level scheme proposed by Urkedal and Hamamoto [9]. The assignment of negative parity for the 208-keV level is supported by the angular distribution measurements of transitions within and out of the rotational band built on this state, as highlighted in Fig. 3. Distributions for the 598 and 908-keV transitions are $L = 2$ in character, implying $J = 7/2$ and $11/2$ for the associated levels. Figure 4(b) shows the angular distribution for the $11/2 \rightarrow 9/2^+$, 954-keV transition. The fit is consistent with the transition being pure $L = 1$, as would be expected for an assignment of $J^\pi = 11/2^-$ for the 1714-keV level, and negative parity for the states at 806 and 208 keV.

Beginning again with the established assignment of $J^\pi = 5/2^+$ for the 670-keV level, Fig. 4(c) shows the measured angular distribution for the 263-keV transition to the 407-keV level. The solid curve is the fit for a $5/2^+ \rightarrow 5/2, L = 1$ decay; the dashed curve shows a $5/2^+ \rightarrow 3/2, L = 1$ decay. Note, however, that a mixed $E2/M1, 5/2^+ \rightarrow 3/2^+$ decay cannot be strictly ruled out. The distribution of the 397-keV transition from the 407-keV level [Fig. 4(d)] is consistent with the $5/2^- \rightarrow 1/2^-$ assignment for a pure quadrupole decay. This 10-keV level is populated from both the 208 and 407-keV states and decays by an $E2$ transition that is highly converted and absorbed, so was not directly observed. However, the 208- and 407-keV states both have ground-state and first-excited branches, so the level energy can be inferred without direct measurement. The assignment of $J^\pi = 1/2^-$ for the 10-keV state is supported by a comparison with low-lying states in ^{73}Br [20].

A more regularly spaced rotational sequence is built on the 670-keV level. The first member of the band is at 892 keV. The in-band decay of 222 keV is consistent with an $E2/M1$ decay having a mixing ratio of $\delta = 0.12(5)$. This is shown by the solid curve in Fig. 4(e). The assignment of $9/2^+ \rightarrow 5/2^+$ via a pure $L = 2$ decay, as indicated by the dashed curve in the figure, is ruled out. Another branch from this state, of 277 keV, helps constrain the 615-keV level to two possible spin hypotheses. The distributions are consistent with either another $J \rightarrow J$ pure dipole transition followed by a quadrupole decay, leading to a $J^\pi = 7/2^-$ assignment [shown as a solid curve in Fig. 4(f)], or the reverse sequence, with a quadrupole transition first (shown as a dashed curve in the same panel). The latter sequence is favored as it would explain the absence of a decay branch from the isomer and is similar to the decay branches of the analogous state in neighboring ^{73}Br [20].

Building on this new basis, the decay scheme was developed to high spin. Although several cascades of transitions were

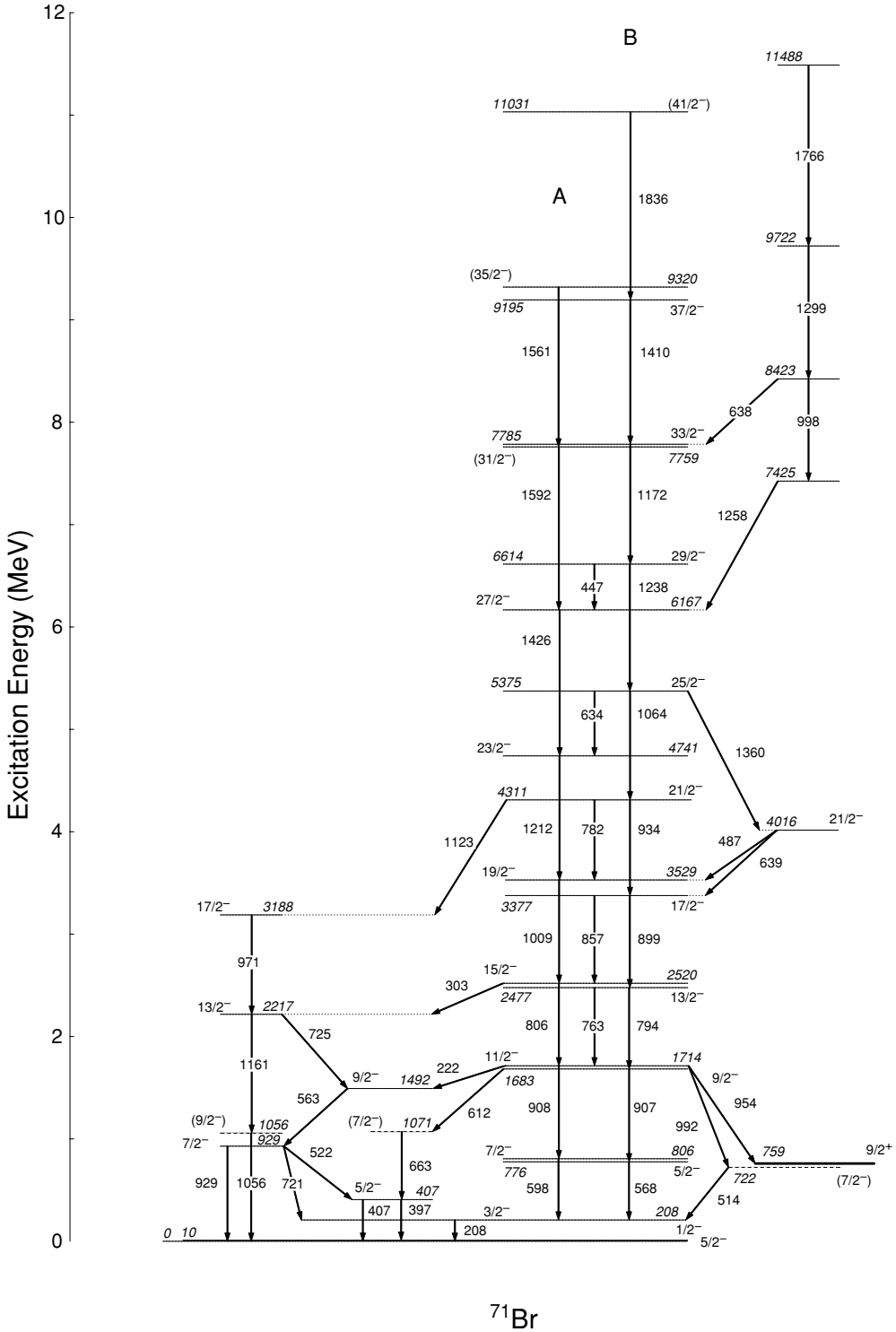

FIG. 5. The negative-parity states inferred from this work for ^{71}Br. Table I contains the details about these transitions and the states from which they decay.

found, none were trivially developed in simple bands. The many interband transitions made the grouping of states into rotational bands unusually difficult. The resultant scheme is sufficiently complicated that we must present the negative- and positive-parity patterns separately in Figs. 5 and 6. Six long cascades of stretched $E2$ transitions could be grouped into distinct bands. For identification purposes we label them "A" to "F." In Sec. IV B we discuss their underlying structure. Substantial "forking" into different structures at high spin was observed in almost all of the sequences, as has been

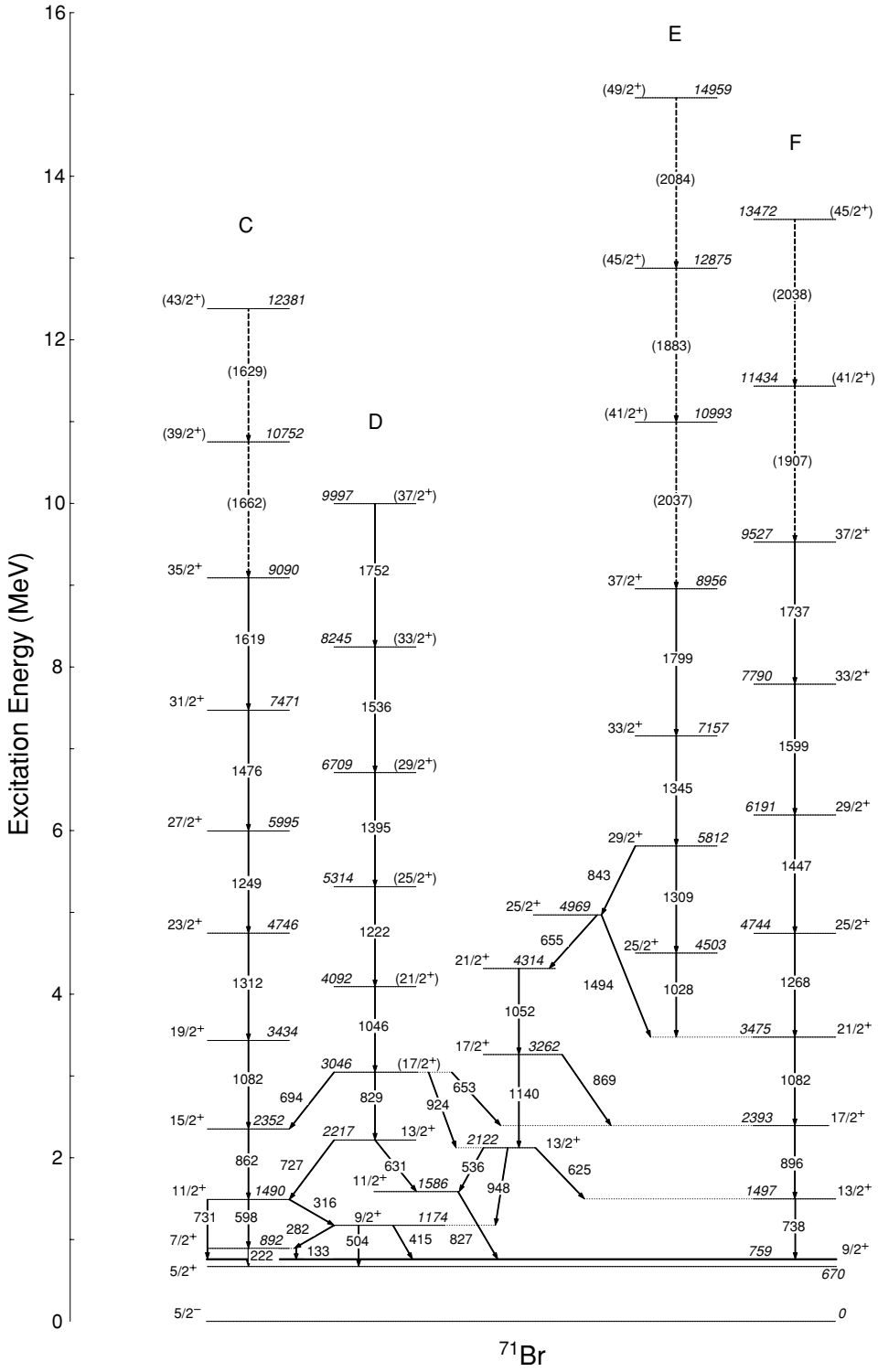

FIG. 6. The composite decay scheme for positive-parity states in ^{71}Br. Table I contains the details of all the transitions in this scheme.

seen in most of the neighboring even-even nuclei [13]. This forking is indicative of shape instability, with the Coriolis force inducing shape changes, usually driven by particle alignment. Once the level sequences were properly established the cross-linking decays were very useful in firmly ordering the states, but initially they confused the intensity balances and made the spectra appear complicated. Figure 7 illustrates this fragmentation in the strongest negative-parity sequence, a $K^\pi = 3/2^-$ band built on the 208-keV level. The data were sufficiently good to extend the decay scheme to $J \geqslant 41/2$. The band is highly signature split at lower spins. The $J^\pi = 11/2^-$ member of this band at 1714 keV has decay branches to four other bands and is critical in constraining many decay paths, as it links together the structures.

The positive-parity sequences can be built up from the $J^\pi = 9/2^+$ 759-keV isomer and the $J^\pi = 5/2^+$ state at

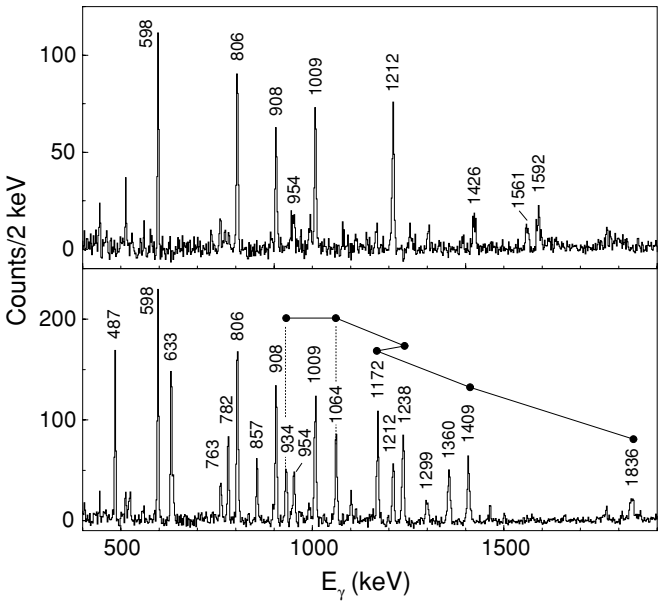

FIG. 7. Sums of $\gamma\gamma$ gates selected to highlight transitions in the negative-parity $K = 3/2$ sequences A (upper panel) and B (lower panel) of ^{71}Br. The filled circles in the lower panel are included to identify the quadrupole transitions within sequence B.

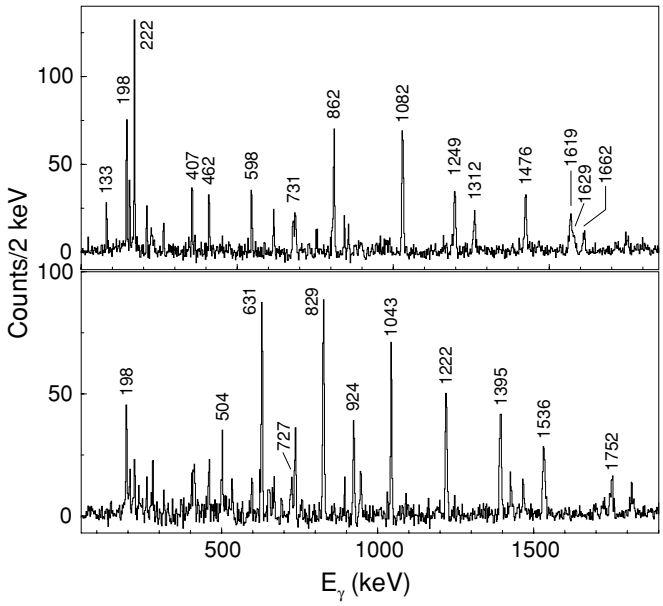

FIG. 8. Sums of $\gamma\gamma$ gates selected to highlight transitions in the $K = 5/2$ positive-parity sequences C (upper panel) and D (lower panel) of ^{71}Br. Note that the intensity patterns, particularly for the upper panel, are somewhat misleading, as a number of $\gamma\gamma$ gates were excluded because of the presence of energy doublets.

670 keV to which it decays. The $K^\pi = 5/2^+$ band is the most regularly spaced structure in ^{71}Br, showing well-behaved strong coupling especially at low spin. Representative spectra are shown in Fig. 8. The states built on the isomer show strong forking and a more irregular structure at lower energies but are disconnected from the rest of the decay pattern at higher energies, resulting in relatively simple spectra. For instance, as displayed in Fig. 9, band "F" is the only sequence observed for which the characteristic pattern of a rotational band is immediately evident.

IV. DISCUSSION

A. β decay

With the new decay scheme for ^{71}Br (Fig. 3) the β decay of ^{71}Kr needs to be revisited. Oinonen *et al.* [10] reported β decay to the ground state (or ground- and 10-keV states) and the 208-keV level but no others, and the inferred $J^\pi = 5/2^-$ for the parent ground state. Their failure to observe β decay to the 262-keV level (the key observation that motivated the Urkedal and Hamamoto work) is now accounted for as we have excluded the existence of the state. Careful examination of Fig. 1 of their paper [10] indeed shows that the 407-keV level was in fact populated in β decay, with both the 407- and 397-keV lines visible in the short-time-bin spectrum, with a similar branching ratio to our current study, and decaying away with a half-life similar to the 198/208 doublet. From their spectrum, the 407-keV level appears to be populated with a similar intensity to the 208-keV state, that is, about a 15% branch. In fact, the new 199-keV transition linking the 407- and 208-keV levels moves some of the excited state population up to the higher level. In addition, population of the 615-keV level cannot be completely excluded, as its 208- and 407-keV decays are degenerate with transitions already identified in the ^{71}Kr decay.

It was noted [10] that the β decay to excited states in this $A = 71$ mirror pair is surprisingly large, as the decay of the $T_z = -1/2$ mirror partner usually decays almost exclusively to

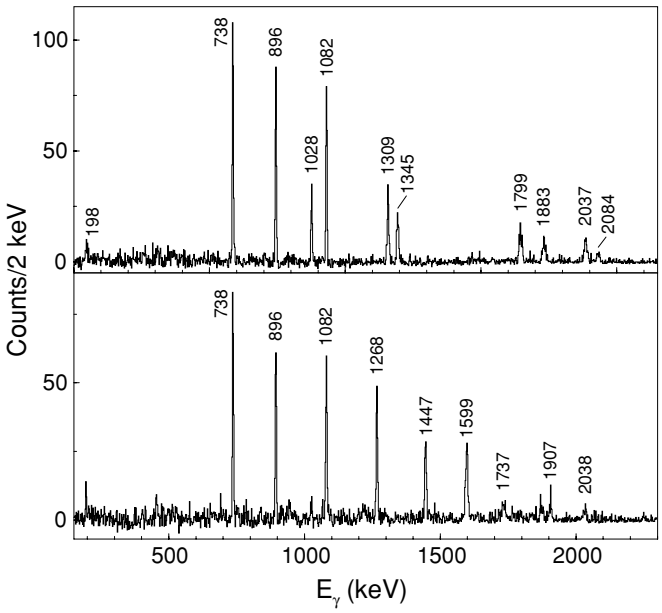

FIG. 9. Sums of $\gamma\gamma$ gates selected to highlight transitions in the $K = 9/2$ positive-parity sequences E (upper panel) and F (lower panel). Note that band E decays directly into the $21/2^+ \rightarrow 17/2^+$, 1082-keV transition of band F.

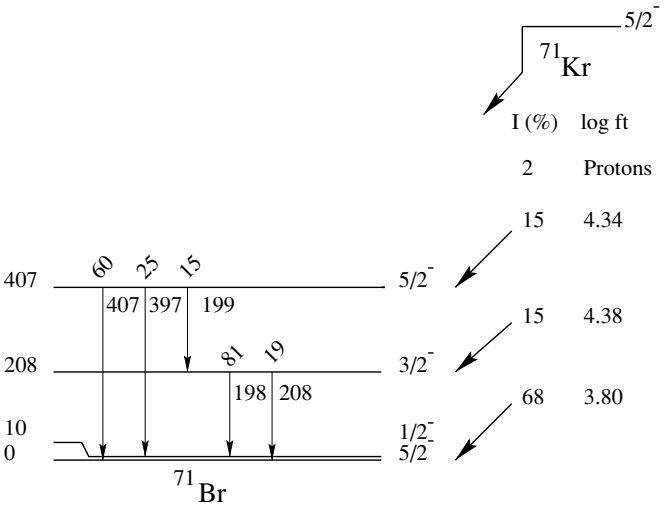

FIG. 10. The modified β-decay scheme for ^{71}Kr.

its analog state in the $T_z = +1/2$ daughter, because of the large overlap of their wave-functions. With our new information the excited state population becomes even larger, with more than 30% going to excited states. This is more than triple that of ^{67}Se [21] and an order of magnitude larger than lighter mirror pairs in the *fp* and *sd* shells. Because the ground state and 407-keV state have the same spin and parity, a population mechanism can now be suggested arising from shape coexistence. Figure 10 shows the β-decay scheme for ^{71}Kr, revised in the light of the measurements in this work.

Our greatly extended decay scheme conflicts with the suggestions of Urkedal and Hamamoto [9] that the ^{71}Kr ground state has $J^\pi = 3/2^-$. Their hypothesis was based on assuming the ^{71}Br low-lying doublet had $J^\pi = 5/2^-$ and $3/2^-$, a situation that was inverted in ^{71}Kr. In our decay scheme the low-lying doublet is fixed at $5/2^-$ and $1/2^-$ as originally suggested by Arrision *et al.* [11]. If the order were reversed in ^{71}Kr, the ground state would become $J^\pi = 1/2^-$, and the decay would proceed almost entirely to the ^{71}Br 10-keV state, with very little population of the $J^\pi = 5/2^-$ levels. The branch to the 407-keV level would be a second forbidden decay, inconsistent with the relatively low log(ft) value of 4.38. Thus, this inversion can be excluded and the expectations of mirror symmetry, that is, a $J^\pi = 5/2^-$ assignment for ^{71}Kr, remains entirely consistent with this work. Were the ^{71}Kr ground-state $J^\pi = 3/2^-$, one would expect the main β-decay branch to proceed to the 208-keV level (presumably the mirror state), with $>8\%$ of the flux, and with smaller branches to the $J^\pi = 5/2^-$ states at 0 and 407 keV. Although we cannot yet rigorously exclude a $J^\pi = 3/2^-$ assignment for the ^{71}Kr ground state, it appears very unlikely. It would also involve a very substantial relative Coulomb shift of $\geqslant$200 keV, which is much larger than expected mirror energy differences (MEDs) that have been measured at low spin in $T = 1/2$ nuclei. In view of this study we expect that a more sensitive β-decay investigation will show population of some of the four $J^\pi = 7/2^-$ states at around 800 keV, rigorously removing all uncertainty of the ground-state spin of ^{71}Kr.

The β-branching ratio to the two $J^\pi = 5/2^-$ states in ^{71}Br at 0 and 407 keV provides direct information on the degree of mixing between the two states and also the difference in admixtures in the ground state of ^{71}K compared to ^{71}Br. This is most easily visualized in a simple two-level mixing model, assuming that there exist two $J^\pi = 5/2^-$ states in each nucleus, each pair having quite different structure, perhaps prolate and oblate, so the "cross" matrix elements measuring the overlap of prolate and oblate states is very small. If the mixing of states in bromine were complete, such that each level was a 50/50 mixture of shapes, and if there were no mixing at all in the krypton ground state (so it were either pure oblate or pure prolate), then the fragmentation would be maximal, with the decay flux equally split between ground and excited states, as the decay picks up the part of each wave-function with which it has large overlap. Similarly, compete mixing in the krypton ground state and no mixing between the bromine levels would also lead to an equal split of flux. However, at the other limit, if the mixing in both nuclei were identical, then orthogonality determines that the ground state of krypton would only decay to the ground state of bromine.

In fact, the experimental situation is intermediate. Although 17% of the β-decay flux to $J^\pi = 5/2^-$ states goes to the 407-keV level of ^{71}Br, and the rest to the ground state, this is slightly biased by phase space, which favors the higher energy decay channel. Applying a small correction to account for this raises the 407-keV state branch to 18%. To proceed further requires recourse to models, as the experimental β-decay data alone is insufficient. A calculated potential energy surface [22] indicates that the ^{71}Kr ground state is oblate with $\epsilon_2 = -0.35$ and having an excited prolate minimum at 600 keV with an axial barrier of $\sim$2.9 MeV. Similar calculations considering triaxiality [23] indicate the barrier in the triaxial direction is lower, about $\sim$1 MeV. In contrast, ^{71}Br is predicted to have a slightly lower axial barrier, about 0.6 MeV less, and be softer in the triaxial direction. Thus, a scenario with ^{71}Kr having a pure oblate ground-state shape, and ^{71}Br with a ground state of 82% oblate and 18% prolate mixture, would reproduce the observed β-branching ratio to the $J^\pi = 5/2^-$ states, although this is not a unique description. A locus of possible mixing solutions can account for the observation. What is unambiguous is the fact that the ground-state wave functions of the mirror pair cannot be the same. In this simple model we can also infer that the mixing matrix element between oblate and prolate shapes in ^{71}Br is quite large, of the order of 50 keV, to account for this mixing of $J^\pi = 5/2^-$ levels 400 keV apart. The mixing has a repulsive effect, pushing the two states apart. This mixing must be different in krypton and bromine, but it appears to not be sufficiently different to cause an inversion with the $J^\pi = 1/2^-$ state in either case. It will be very interesting in the future to try to identify the mirror excited states in ^{71}Kr and explore this mixing issue more quantitatively. Finding the $J^\pi = 5/2^-$ excited state in ^{71}Kr would be particularly important for understanding this issue.

For completeness, we should consider the experimental consequences of an inversion of the ground-state doublet in ^{71}Kr, such that the $J^\pi = 1/2^-$ state lies a few keV below the $J^\pi = 5/2^-$ level. In that case, both levels could have substantial β-decay branches. If the two half-lives were quite close,

probably within a factor of 2, it would be easy to mistake the decays reported by Oinonen *et al*. [10] as coming from a single state. The $J^\pi = 5/2^-$ state would decay to the corresponding levels in ^{71}Br, and to the 207-keV $J^\pi = 3/2^-$ level, whereas the $J^\pi = 1/2^-$ state would decay to the corresponding 10-keV state in ^{71}Br (which would be unobserved) and the 208-keV level (which would be masked by the upper decay). It would involve some serendipity, as were the states more than a few keV apart the upper state would γ decay to the lower, and some fine-tuning would be needed to match the half-lives. However, the higher spin state usually receives most of the population from reactions, so such inversion would be difficult to detect in β decay. It could conceivably account for the different half-lives reported for ^{71}Kr [3,24] because one was measured following spallation and one from fragmentation. Only an in-beam study of ^{71}Kr will resolve this issue. As we have seen from ^{71}Br several excited states decay to both members of the low-lying doublet and fix their relative position.

B. Band assignments and shapes

Candidates for eight distinct Nilsson configurations have been found in the first 800 keV of excitation in ^{71}Br. There is much similarity with neighboring bromine isotopes ^{73,75,77}Br [20,25–29], especially with ^{75}Br [27]. The experimental measurements of magnetic moments of light bromine isotopes using low-temperature nuclear orientation is valuable in understanding the trends. Griffiths *et al*. [30] performed extensive particle-triaxial-rotor calculations that allowed the structural evolution to be followed. The deformation was predicted to increase with decreasing neutron number, and in the lightest isotopes the level sequence could only be explained by invoking oblate shapes. These findings are in agreement with our empirical observations.

A major difference among the bromine isotopes is the relative position of the positive-parity states (based in the $g_{9/2}$ shell model orbit) relative to the ground state. In ^{71}Br there is a 670-keV gap, whereas in ^{73}Br it is 286 keV, in ^{75}Br 132 keV, and in ^{77}Br only 106 keV. There may be more than one mechanism causing this effect. This sequence of bromine isotopes spans a region of changing shapes. In the lightest bromine isotopes, centered on ^{70}Br, there is a region where oblate ground states are favored, stabilized by gaps in the single-particle sequence at nucleon number 34 and 36, but with relatively low-lying prolate bands. With increasing neutron number, the prolate shell gap at particle number 38 becomes dominant and the oblate states become nonyrast and difficult to observe experimentally. The increasing gap between $g_{9/2}$ and *fp* shell configurations can partly be attributed to favored oblate shapes in the lighter nuclei. However, in addition, the increasing separation may reflect the growing importance of neutron-proton correlations as the $N = Z$ line is approached and may lead to ^{70}Br having a 900-keV gap [31,32] between its highly correlated $J^\pi = 0^+$ ground state and all other excited configurations.

In ^{71}Br, three of the bandheads support rotational structure of both signatures, which extend as high as $J = 49/2$. In all the high-spin structures the rotation is disrupted at $\sim$4 MeV. It is important to note that in the core nucleus, ^{70}Se, two $J = 8$ configurations are known [13,33] near 4 MeV in excitation, the yrast $J = 8$ state being prolate, and the yrare state being oblate. These configurations are quite distinct, as shown by the β decay of the $J^\pi = 9^+$ oblate isomer in ^{70}Br, which decays only to the oblate yrare configuration [34–36], despite phase space favoring decay to the yrast state. The shape polarization is driven by alignment of $g_{9/2}$ particles. Similar shape competition occurs again near spin $J = 16$, when both pairs of protons and pairs of neutrons align.

1. The $J^\pi = 5/2^-$ ground-state band

The first members of a rotational band built on the ground state can be identified at 929, 1056, and 2217 keV. The band has a relatively small moment of inertia, indicating modest deformation, not inconsistent with the near-oblate bands known in this region. Particle-triaxial-rotor calculations [30] indicate the close-spaced doublet of ground and first-excited states only occurs in a potentional with $\epsilon_2 \geqslant 0.2$ and $\gamma = 60^\circ$, that is, for oblate shapes. The ground-state wave function in this model was calculated to be mainly from the $[312]5/2^-$ Nilsson state, with smaller admixtures from 5/2 members of other rotational bands. The band shows considerable signature splitting, a feature often associated with triaxiality or band mixing. The small moment of inertia makes the band become nonyrast rapidly, and only the strong signature splitting of the dominant $K^\pi = 3/2^-$ allows significant population up to the $J = 13/2$ member. In the notation used by the Florida State University (FSU) group [27], this band corresponds to their structure "J" in ^{75}Br.

2. The $J^\pi = 1/2^-$ 10-keV state

No excited states could be firmly associated with this configuration. This is consistent with the band having a similar moment of inertia to the ground-state band, as all the members would be quite nonyrast and so not well populated in this high-spin reaction. For example, the $J^\pi = 5/2^-$ member of the band would lie near 1 MeV and would be the fifth state with this spin. In contrast, if this bandhead had considerable prolate deformation ($\epsilon_2 \sim 0.3$) the $J = 5/2$ member would lie below 600 keV and would likely have been observed in this work. No equivalent state has been identified in ^{75,77}Br, but in ^{73}Br this configuration is the ground state [37], measured in a low-temperature nuclear orientation study and assigned a dominant Nilsson configuration $[310]1/2^-$.

3. The $J^\pi = 3/2^-$ 208-keV band

This is the best developed negative-parity band, showing two clear cascades extending to spin $J^\pi = 41/2^-$, labeled as "A" and "B" in Fig. 5. The moment of inertia is larger than that of the ground-state band and is consistent with the near-prolate bands found in neighboring nuclei. For example,

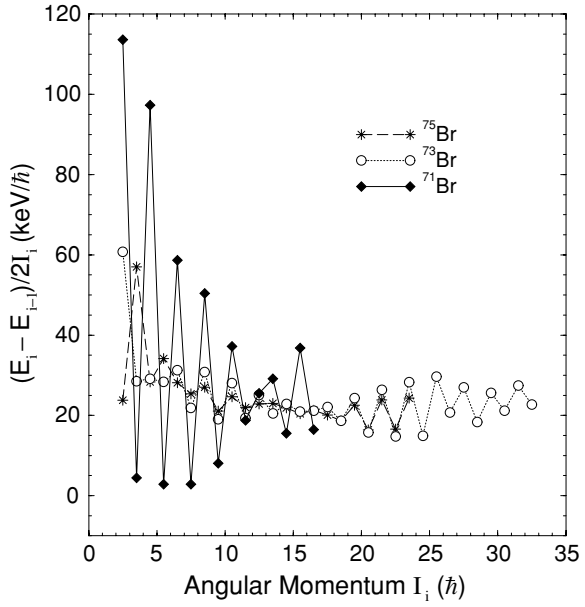

FIG. 11. Signature splitting in the $K = 3/2$ negative-parity bands in ^{71,73,75}Br.

the corresponding band in ^{73}Br has been identified [20,25] as being prolate with large deformation, $\epsilon_2 = 0.38$, based on lifetime measurements, with an asymptotic Nilsson configuration $[312]3/2^-$ and stabilized by the $N = 38$ deformed gap. The bands in ^{73,75}Br ($N = 38, 40$) have very similar moments of inertia, and presumably deformation. A comparison of these bands is shown in Fig. 11. Particle-triaxial-rotor calculations [30] show there is an evolution of the dominant component in the Nilsson wave function with decreasing neutron number, starting with $[301]3/2^-$ near stablility and becoming nearly pure $[312]3/2^-$ in ^{71,73}Br. This trend is driven by increasing deformation, predicted to be $\varepsilon \geqslant 0.3$ in the lightest isotopes. However, the band we find in ^{71}Br shows dramatic signature splitting, which is usually indicative of triaxiality. This splitting is much larger than in the neighboring isotopes. Although the band has quadrupole cascades of both signatures (Fig. 5) with several linking $\Delta J = 1$ transitions, it is far from a traditional deformed band with a fixed moment of inertia, as can be seen from Fig. 12. In Fig. 12(a) the favored signature cascade $(3/2, 7/2, 11/2, \ldots)$ is compared with the equivalent band in neighboring bromine isotopes. ^{71}Br is the most irregular with a very steep initial rise. This rapid increase is found in several neighboring nuclei and arises from oblate-prolate shape coexistence, with prolate configurations becoming increasingly favored with rotation owing to their larger moments of inertia. The moment of inertia of this band is also compared to the $N = 36$ isotone, ^{70}Se, in Fig.12(b) where shape coexistence has been studied in detail [33]. At the highest spins the downsloping trajectory is indicative of a band approaching noncollective oblate termination.

Figure 11 shows that above $J^\pi = 19/2^-$ the signature splitting in ^{71}Br decreases dramatically so the band becomes more regularly spaced and like its neighbors. There is also an

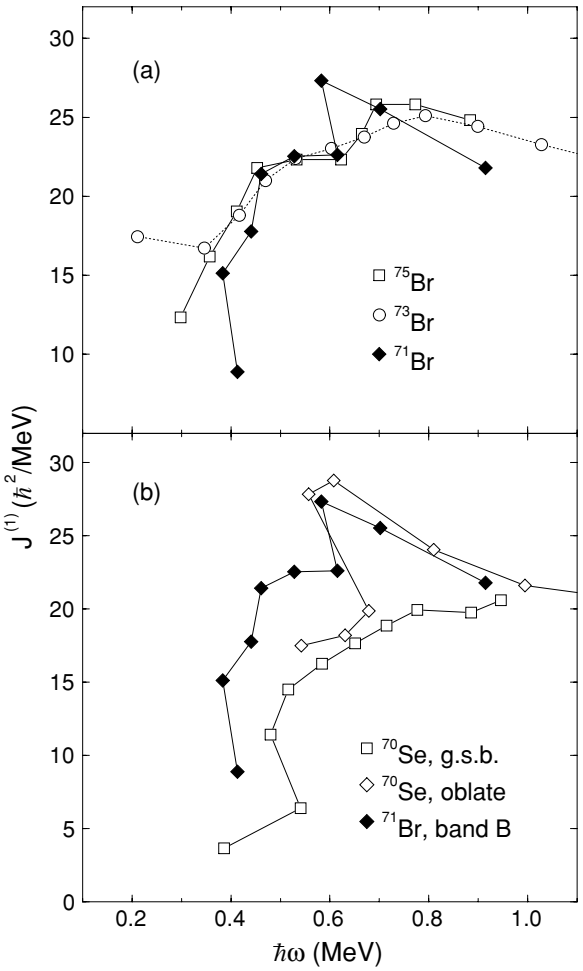

FIG. 12. A comparison of the kinematic moments of inertia of the favored signatures of the negative-parity band in ^{71}Br (band "B" of this work) with (a) the analogous bands of the neighboring odd-A bromines, and (b) with the ground-state and oblate excited bands in ^{70}Se.

inversion of signature splitting, further indicating a change in structure. The spin at which these changes occur corresponds to that of a three-quasi particle configuration coupling the $J^\pi = 3/2^-$ proton to a fully aligned pair of $g_{9/2}$ nucleons. Such alignments are known to drive shape changes in soft nuclei in this region, and a move to a more prolate shape would account for the decrease in signature splitting. Another three-quasi particle structure has a bandhead at 4016 keV and probable spin and parity $J^\pi = 21/2^-$ that decays into the $K = 3/2$ band. These levels in ^{71}Br appear similar to their ^{70}Se neighboring isotone, where oblate and prolate configurations compete near the yrast line above ~4 MeV. This similarity is shown in Fig. 12, which compares the moment of inertia of the favored signature sequence to the bands in ^{70}Se. Here, in ^{71}Br, the prolate configuration is coupling into the continuation of the $K = 3/2$ band, reducing the triaxiality, and thus the signature splitting, whereas the oblate state forms a distinct and energetically favored bandhead. No clear rotational structure could be directly observed above the 4016-keV state, although a higher lying cascade feeding the main band may be related.

4. The $J^\pi = 5/2^-$ 407-keV band

States at 1071 and 1492 keV are candidate members of this band, based on their positions and possible spins. However, they are clearly mixed with other configurations, as they have strong out-of-band links to the other negative-parity sequences. Comparing the $7/2 \rightarrow 5/2$ transitions in the two $J = 5/2$ bands suggests the 407-keV band has a considerably larger moment of inertia, though the large signature splitting makes this indicator far from conclusive. If these states are indeed rotational members of this band, it appears to have a moment of inertia similar to that of the 208-keV band, that is, consistent with a prolate deformed shape. In calculations [9,30] there is only one $J^\pi = 5/2^-$ level near the Fermi surface, so the observation of two low-lying states with the same spin and parity is a strong indicator of shape coexistence, with the valence proton coupling to oblate and prolate cores, respectively.

5. The $J^\pi = 5/2^+$ 670-keV band

The first members of this band at 892, 1174, 1490, 2217, and 2352 keV represent the most regular strong-coupling rotational sequence in ^{71}Br, labeled as "C" and "D" in Fig. 6. This band has very close similarity to analogous bands in ^{73,75}Br [20,25,27], although surprisingly the unfavored signature cascade in ^{73}Br has not been found. It has been assigned as the prolate Nilsson [422]$5/2^+$ configuration, driven by the highly prolate polarizing $K = 5/2$ projection of the $g_{9/2}$ orbit. The band is perturbed considerably at low spin by interaction with the decoupled $J^\pi = 9/2^+$ sequence, which has only one signature, and by the oblate sequence built on the isomer. Consequently, the $J = 13/2$ and $J = 17/2$ states are pushed up by mixing. The "shift" caused by this mixing can be estimated as $\sim$300 keV if a constant moment of inertia is assumed. There are three states of spin $J = 13/2$ lying within 700 keV of each other, so the unperturbed positions must be quite close, and the mixing almost complete. At higher spin the mixing diminishes and the band becomes regularly spaced with near-constant moment of inertia. In ^{75}Br the disruption caused by mixing is even more severe [27], but it appears that structures identified as "B" and "C" by the FSU group are most closely associated with this band.

6. The $J^\pi = 9/2^+$ 759-keV bands

An inspection of the Nilsson diagram shows that a low-lying $J^\pi = 9/2^+$ isomer arises when the nucleus is polarized to an oblate shape. Collective rotation of oblate shapes is not energetically favored owing to the corresponding small moment of inertia. The series of positive-parity states that could originate from true oblate rotation [at 1586 keV ($J = 11/2$), 2122 keV ($J = 13/2$), 3262 keV ($J = 17/2$), and 4314 keV ($J = 21/2$)] is heavily mixed and poorly populated. A more strongly populated cascade appears to have only one signature and has a considerably larger moment of inertia. This configuration probably comes from the $g_{9/2}$ valence particle becoming rotationally aligned, in a well-deformed prolate potential. These structures compete for population near the bandhead. By $J = 17/2$ the oblate candidate is nonyrast by 869 keV. The long sequence of rotationally aligned states is unusual at high spin as it has two cascades of states (labeled as "E" and "F" in Fig. 6) apparently with the same spin and parity, both populated over a wide spin range. This behavior is best interpreted in the context of the ground-state sequences in even-even core nuclei ^{72}Kr and ^{70}Se [13]. In these nuclei a very unusual situation arises where two different shaped configurations compete as the yrast states. One set of levels corresponds to the continuation of large-deformation prolate rotation; the other, an oblate set of levels moving toward fully aligned termination, is much less collective. Figure 13 is the most clear-cut way of comparing these bands, showing the Routhians (relative excitation energies in a fixed-deformation reference frame). It can be seen that ^{71}Br indeed looks similar to its even-even neighbors. One subtle difference concerns blocking of orbits and the delay of alignments. In $N = Z$ ^{72}Kr the protons and neutrons occupy the same orbits, so experience identical Coriolis forces, and show pair-breaking alignments at one characteristic frequency. In ^{71}Br, the situation is a little more complicated, in that the unpaired proton sits above the

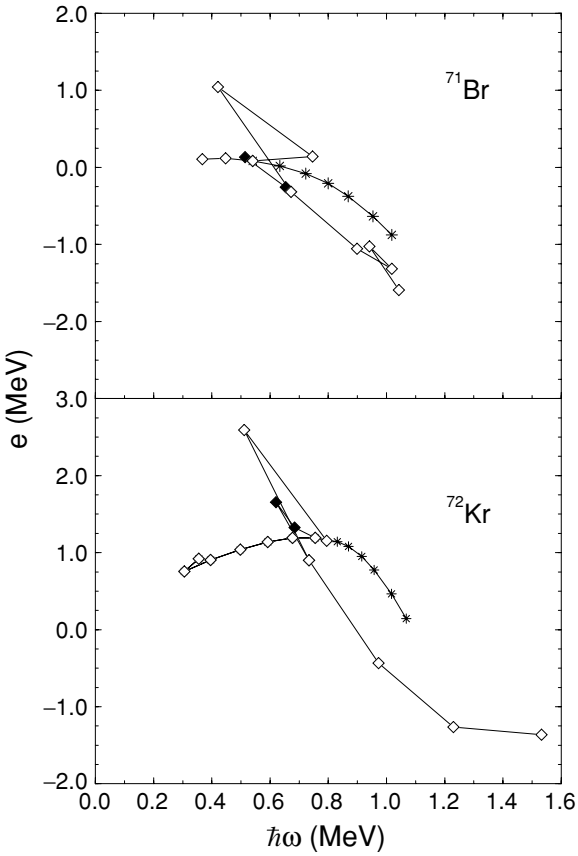

FIG. 13. The Routhian (energy in the rotating frame of reference) for the positive-parity states built on the $J^\pi = 9/2^+$ isomer, showing the strong similarity with neighboring $N = 36$ isotone, ^{72}Kr, where high-spin shape changes have been documented [13]. The open diamonds in the top panel correspond to sequence "E" and the stars to sequence "F." The Harris parameters are $J_0 = 17.5$ and $J_1 = 0$.

Fermi surface and blocks the natural proton alignment, so more rotational energy is required before alignment can occur. From Fig. 13 it can be seen that this blocking does not influence the overall topology, and the neutron alignment alone is enough to drive the shape changes. At the very highest frequencies, near 1 MeV of rotational energy, evidence for a delayed proton alignment is clear. Total Routhian surface calculations indicate that such a delayed crossing (almost double the normal prolate crossings in the region) can only occur for an oblate-deformed shape.

V. CONCLUSION

The ^{71}Br decay scheme has been investigated in detail. The low-lying decay scheme has been revised, and many spins and parities have been rigorously established. Candidates for eight Nilsson bandheads have been located and several rotational bands have been established, some to high spin ($J \geqslant 20\hbar$). The bands have considerably different moments of inertia, indicating softness of the core, which is easily polarized by occupancy of individual neutron Nilsson states. The firm assignment of spins to the low-lying levels has allowed the β decay of ^{71}Kr to be reconsidered. The experimental evidence is consistent with ^{71}Kr having a $J^{\pi} = 5/2^{-}$ ground-state spin as is the expectation for the mirror partner of ^{71}Br. The unusually strong β decay to excited states between this mirror pair seems to arise from the strong mixing of shapes and implies that the wave functions of the ^{71}Kr and ^{71}Br ground states must be different from each other. An investigation of excited states of ^{71}Kr could provide the necessary additional information to quantify this difference and hence the degree of mirror distortion.

ACKNOWLEDGMENTS

The operation of Gammasphere requires continuous attention and we would like to thank the Argonne group of Robert Janssens, Mike Carpenter, Torben Lauritsen, and John Rohrer for their assistance and dedication to keeping the device working at its top performance level. High-quality calcium targets were essential in this work and we would like to thank John Greene of ANL for their preparation. We would like to acknowledge important discussions with Stefan Frauendorf of the University of Notre Dame concerning shape mixing and β decay. This research was supported in part by the U.S. Department of Energy Office of Nuclear Physics under Contract Nos. W-31-109-ENG-38 and FG02-88ER-40406, by Research Corporation Grant No. CC5166, and by National Science Foundation Grants Nos. PHY95-14157, and PHY-0244895.

[1] J. B. Ehrman, Phys. Rev. **81**, 412 (1951).
[2] R. G. Thomas, Phys. Rev. **88**, 1109 (1952).
[3] R. Pfaff, D. J. Morrissey, W. Benenson, M. Fauerbach, M. Hellstrom, C. F. Powell, B. M. Sherrill, M. Steiner, and J. A. Winger, Phys. Rev. C **53**, 1753 (1996).
[4] B. Blank *et al*., Phys. Rev. Lett. **74**, 4611 (1995).
[5] E. Nolte, Y. Shida, W. Kutschera, R. Prestele, and H. Morinaga, Z. Phys. **268**, 267 (1974).
[6] S. M. Fischer, D. P. Balamuth, P. A. Hausladen, C. J. Lister, M. P. Carpenter, D. Seweryniak, and J. Schwartz, Phys. Rev. Lett. **84**, 4064 (2000).
[7] E. Bouchez *et al*., Phys. Rev. Lett. **90**, 082502 (2003).
[8] W. D. Myers and W. J. Swiatecki, Nucl. Phys. **81**, 1 (1966).
[9] P. Urkedal and I. Hamamoto, Phys. Rev. C **58**, 1889(R) (1998).
[10] M. Oinonen *et al*., Phys. Rev. C **56**, 745 (1997).
[11] J. W. Arrison, T. Chapuran, U. J. Huttmeier, and D. P. Balamuth, Phys. Lett. **B248**, 39 (1990).
[12] T. Martinez. *et al*., Laboratori Nazionali di Lenaro, 1997 Annual Report, LNL-INFN Report No. 125/98, p. 8.
[13] S. M. Fischer, C. J. Lister, and D. P. Balamuth, Phys. Rev. C **67**, 064318 (2003).
[14] N. S. Kelsall *et al*., Phys. Rev. C **65**, 044331 (2002).
[15] I. Y. Lee., Nucl. Phys. **A520**, 641 (1990).
[16] D. G. Sarantites, P.-F. Hua, M. Devlin, L. G. Sobotka, J. Elson, J. T. Hood, D. R. LaFosse, J. E. Sarantites, and M. R. Maier, Nucl. Instrum. Methods A **381**, 418 (1996).
[17] D. C. Radford, Nucl. Instrum. Methods A **361**, 297 (1995).
[18] P. M. Endt, At. Data Nucl. Data Tables **23**, 547 (1979).
[19] E. Hagberg, J. C. Hardy, H. Schmeing, H. C. Evans, U. J. Schrewe, V. T. Koslowsky, K. S. Sharma, and E. T. H. Clifford, Nucl. Phys. **A383**, 109 (1982).
[20] J. Heese *et al*., Phys. Rev. C **36**, 2409 (1987); **41**, 1553 (1990).
[21] P. Baumann *et al*., Phys. Rev. C **50**, 1180 (1994).
[22] P. Moller and J. R. Nix, At. Data Nucl. Data Tables **26**, 165 (1981).
[23] S. Aberg, Phys. Scr. **25**, 23 (1982).
[24] B. Blank, Eur. Phys. J. A **15**, 121 (2002).
[25] C. Plettner *et al*., Phys. Rev. C **62**, 014313 (2000).
[26] L. Luhmann, M. Debray, K. P. Lieb, W. Nazarewicz, B. Wormann, J. Eberth, and T. Heck, Phys. Rev. C **31**, 828 (1985).
[27] G. Z. Solomon, G. D. Johns, R. A. Kaye, and S. L. Tabor, Phys. Rev. C **59**, 1339 (1999).
[28] G. N. Sylvan, J. E. Purcell, J. Doring, J. W. Holcomb, G. D. Johns, T. D. Johnson, M. A. Riley, P. C. Womble, V. A. Wood, and S. L. Tabor, Phys. Rev. C **48**, 2252 (1993).
[29] J. Doring, L. Funke, R. Schwengner, and G. Winter, Phys. Rev. C **48**, 2524 (1993).
[30] A. G. Griffiths, C. J. Ashworth, J. Rikovska, N. J. Stone, J. P. White, I. S. Grant, P. M. Walker, and W. B. Walters, Phys. Rev. C **46**, 2228 (1992).
[31] D. G. Jenkins *et al*., Phys. Rev. C **65**, 064307 (2002).
[32] G. de Angelis *et al*., Eur. Phys. J. A **12**, 51 (2001).
[33] G. Rainovski *et al*., J. Phys. G **28**, 2617 (2002).

[34] E. Roeckl, Nucl. Phys. **A704**, 200 (2002).
[35] A. Piechaczek, E. F. Zganjar, J. C. Batchelder, B. D. MacDonald, W. D. Kulp, S. D. Paul, R. Terry, and J. L. Wood, Phys. Rev. C **62**, 054317 (2000).
[36] M. Karny, L. Batist, D. Jenkins, M. Kavatsyuk, O. Kavatsyuk, R. Kirchner, A. Korgul, E. Roeckl, and J. Zylicz, Phys. Rev. C **70**, 014310 (2004).
[37] N. J. Stone *et al*., in *Nuclear Physics of the Zirconium Region*, edited by J. Ebeth, R. A. Mayer, and K. Sistemich (Springer, Berlin, 1988), p. 309.